www.dergipark.gov.tr
ISSN:2148-3736
El-Cezerî Fen ve Mühendislik Dergisi
Cilt: 9, No: 1, 2022 (159-170)

El-Cezerî Journal of Science and Engineering
Vol: 9, No: 1, 2022 (159-170)
DOI :10.31202/ecjse.952728

ECJSE

Research Paper / Makale

Design and Kinematic Analysis of Proposed Adaptive Landing Gear for Multirotor UAV

Nihat ÇABUK[1a]

Vocational School of Technical Sciences, Aksaray University, Aksaray, TURKIYE
nihatcabuk@aksaray.edu.tr

Received/Geliş: 15.06.2021 **Accepted/Kabul:** 22.12.2021

Abstract: One of the weaknesses of multi-rotor unmanned aerial vehicles (UAVs) or vertical take-off and landing aircraft is that they need a flat surface to make a safe landing. In order to reduce the impact of this weakness, it is inevitable to add systems that will give the UAV some additional capabilities related to landing capability. In this study, a four-arm adaptive landing gear is designed and kinematically analyzed for a multi-rotor UAV. The adaptability feature is achieved by positioning the arm ends relative to the uneven ground by automatically changing the angles of the revolute joints so that the vehicle can land safely on uneven ground. The joint angles of the adaptive landing gear, which consists of four robotic arms, each with two joints, are changed by the controller depending on the distance information received from the ultrasonic distance sensor. This distance information is evaluated in the controller according to the determined algorithm and the required angle values of the joints are determined. Within the scope of this study, a scaled adaptive landing gear was designed for an eight-rotor UAV whose mathematical model was also obtained. According to proposed landing gear, which consists of four arms with two limbs, each with a length of 200 mm, the maximum angle of inclination of the uneven ground on which the UAV can land safely is calculated as 44.5°. In addition, the motion trajectory of the end point of the arm, which is the part of the arm that will contact the ground, was obtained with the simulation performed.

Keywords: Safe landing, Adaptive landing gear, UAV, Distance sensor, Kinematic analysis

Çok Rotorlu İHA için Önerilen Uyarlanabilir İniş Takımının Tasarımı ve Kinematik Analizi

Öz: Çok rotorlu insansız hava araçlarının (İHA) veya dikey olarak kalkış ve iniş yapabilen hava araçlarının en zayıf yönlerinden biri güvenli bir iniş gerçekleştirebilmeleri için düz bir zemine ihtiyaç duymalarıdır. Bu zayıflığın etkisini azaltmak için İHA'ya iniş kabiliyeti ile ilgili bazı ek beceriler kazandıracak sistemlerin eklenmesi kaçınılmazdır. Bu çalışmada, çok rotorlu bir İHA için dört kollu adaptif iniş takımı tasarlanmış ve kinematik analizi yapılmıştır. Uyarlanabilirlik özelliği, aracın engebeli zemine güvenli bir şekilde inebilmesi için, dönel olan eklemlerin açıları otomatik olarak değiştirilerek kol uçları engebeli zemine göre konumlanmasıyla elde edilir. Her biri iki eklemli olan dört robotik koldan oluşan adaptif iniş takımının eklem açıları, ultrasonik mesafe sensöründen alınan mesafe bilgisine bağlı olarak kontrolcü tarafından değiştirilir. Bu mesafe bilgisi, belirlenen algoritmaya göre kontrolörde değerlendirilerek eklemlerin gerekli açı değerleri belirlenir. Bu çalışma kapsamında, matematiksel modeli de elde dilen sekiz rotorlu İHA'ya uygun olarak ölçeklendirilmiş adaptif iniş takımı tasarlanmıştır. Her birinin uzunluğu 200 mm olan ikişer uzuvlu dört koldan oluşan bu iniş takımına göre İHA'nın güvenli bir şekilde inebileceği engebeli zeminin maksimum eğim açısı 44.5° olarak hesaplanmıştır. Bunun yanında, gerçekleştirilen simülasyonla kol uç noktasının, ki bu kolun zemine temas edecek kısmı, hareket yörüngesi elde edilmiştir.

Anahtar Kelimeler: Güvenli iniş, Uyarlamalı iniş takımı, İHA, Mesafe sensörü, Kinematik analiz

How to cite this article
Çabuk, N., "*Design and Kinematic Analysis of Proposed Adaptive Landing Gear for Multirotor UAV*" El-Cezerî Journal of Science and Engineering, 2022, 9 (1); 159-170.

Bu makaleye atıf yapmak için
*Çabuk, N., "Çok Rotorlu İHA için Önerilen Uyarlanabilir İniş Takımının Tasarımı ve Kinematik Analizi" El-*Cezerî Fen ve Mühendislik Dergisi 2022, 9 (1); 159-170.
ORCID ID: 0000-0002-3668-7591

1. Introduction

Unmanned aerial vehicles (UAVs) are the most popular aircraft of the new millennium, which can be used for both military and civilian purposes. As the usage areas of these vehicles increase, their equipment also diversifies and vice versa. Examples of these are UAVs with cameras or various sensors, UAVs carrying pesticides for agricultural purposes[1–3], and even UAVs equipped to serve search and rescue activities and/or emergency medical aid. Although not limited to these examples, studies on UAVs are both increasing and diversifying day by day. Thus, it has led to an increase in both the number and variety of studies on them. For example, UAVs with integrated robot arms and grippers to pick up and move an object have also taken their place among the popular study topics of the recent past [4–10]. In addition to all these, it can be seen that both software and hardware studies are used to increase the mission performance of UAVs, although not to fulfill an external task. Studies that offer different solutions about the landing gear, which is one of them and significantly affects the landing performance of the UAV, has become an important research topic since the recent past. In fact, it would not be wrong to say that the landing gear of UAVs is the key equipment for these vehicles to land safely on uneven surfaces. Therefore, it can be said that recently, there has been an increase in studies on dynamic and adaptive landing gear of UAVs.

UAVs with dexterous landing gear or robotic manipulators are some of these study topics. In particular, landing is one of the most critical tasks of almost all aircraft [11]. Manned or unmanned fixed-wing aircraft require larger flat areas for landing, while rotary-wing aircraft do not.

Although rotary wing aircraft are more dexterous in landing and take-off capability, too much slope in the landing area can cause these vehicles to rollover. When some studies to overcome this problem are reviewed, Sarkisov et al. [12] worked on a landing gear consisting of four legs, each with two degrees of freedom. In their experimental work, they showed that the drone can land safely on uneven surfaces. In their study, which is not based on distance measurement, they stated that an optical torque sensor is integrated into the knee joint of each leg so that the UAV can adapt to rough terrain more quickly. Luo et al. [13] worked on a model in which a quadrotor drone had a four-piece landing gear attached to the vehicle for smoother landing. They claimed that they obtained satisfactory results from these landing gear controlled based on artificial neural networks [14,15]. Nadan et. al. [16] analyzed the landing gear, which was inspired by the anatomy of birds. As a result of the experiments, they came to the conclusion that the hexacopter can land and take off over objects of different shapes. Tang et al. [17] worked on an adaptive landing gear system, which is mechanically simpler but uses a control structure based on a depth camera, IMU and optical flow sensor. They stated that they experimentally demonstrated the applicability of the proposed system.

In this study, an adaptive landing gear design and kinematic analysis were performed. Unlike previous similar studies, adaptive landing gear control based on instant measurement of the distance to the ground has been proposed. In addition, the design and modeling of an eight-rotor UAV, in which the designed adaptive landing gear can be integrated, has been made.

In the next part of the study, a solid model of an eight-rotor UAV was created and its mathematical model was obtained. In the following, studies on adaptive landing gear design and kinematic analysis are presented in accordance with this UAV. Finally, the control algorithm and simulation results are presented.

2. Materials and Methods

2.1. Octorotor UAV System

Multi-rotor UAV systems are systems that can control both linear and angular movements by

controlling the angular speeds (Ω_i) of each rotor-propeller pair. Each rotor-propeller pair creates a thrust at certain angular speeds as seen in Equation 1, depending on the characteristics of the rotor and propellers. The proportionality constant (k_f) used to calculate this force (F_i), which is proportional to the square of the angular velocities of this pair, is determined experimentally.

$$F_i = k_f * {\Omega_i}^2 \tag{1}$$

The total thrust (F_t) obtained for the eight-rotor UAV in this study, for *n*=8, is given in Equation 2.

$$F_t = \sum_{i=1}^{n} F_i \tag{2}$$

The angular position relationship between the UAV body and the earth is used to obtain the dynamics of the UAV. Figure 1 shows the body fixed coordinate system [B] and the earth fixed coordinate systems [E].

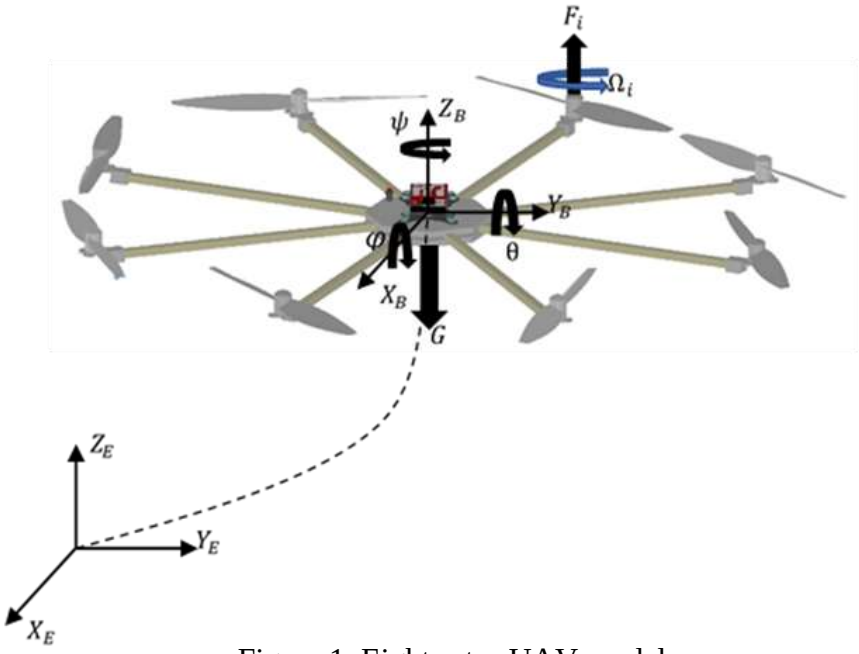

Figure 1. Eight rotor UAV model.

The angular relationship between these two coordinate systems can be represented by Equation 3.

$${}^{B}R_E = R_\varphi * R_\theta * R_\psi \tag{3}$$

Here, R_φ, R_θ and R_ψ are the Euler angles that describe the rotation in the roll pitch and yaw axes, respectively. Considering the obtained rotation matrix ${}^{B}R_E$, the net force acting on the body of the vehicle is obtained as seen in Equation 4.

In this equation, the drag force (F_d) is usually assumed to be zero in order to reduce the complexity of the controller. The net force (F_b) acting on the drone consists of the thrust forces (F_t), gravitational forces (G) and disturbing forces including drag forces.

$$F_b = F_t - ({}^{B}R_E * G + F_d) \tag{4}$$

So, the translational acceleration of the drone is obtained from Equation 5.

$$\dot{V}_b = \frac{F_b}{m} - (\omega_b \text{ x } V_b) \tag{5}$$

In the equation, V_b is the translation velocity in the body frame and $\omega_b = [p\ q\ r]^T$ is the angular velocity vector of the vehicle according to the body frame, respectively. The ω_b value is taken from the Inertial Measurement Unit (IMU). These forces acting on the vehicle can create a moment effect on the vehicle. These moments are the moments in the x and y axes, respectively, expressed as roll-pitch, due to the force difference produced by the propellers. The moment that causes rotation in the z axis, on the other hand, is the reaction moment expressed as yaw, which is dependent on the mechanical properties of the rotors and propellers and occurs in the opposite direction of rotation of the rotors. This torque is also proportional to the square of the angular velocity of the rotors, and this ratio is expressed with a torque constant. This constant, like the force constant, is calculated experimentally. The relationship between the torque, the angular velocity of the rotor and the torque constant is shown by the equation given below.

$$M_i = k_m * {\Omega_i}^2 \tag{6}$$

Since the moment effect of the lifting forces produced by the propellers is related to the geometry of the vehicle, the placement of the propellers according to the coordinate axis on the vehicle body should be known. The relationship between these moments, the forces causing the moments and the angular velocities of the motors causing the forces is established with the matrix Z given in Equations 7-9.

$$\begin{bmatrix} F_t \\ M_r \\ M_p \\ M_y \end{bmatrix} = [Z] * \begin{bmatrix} {\Omega_1}^2 \\ \vdots \\ {\Omega_8}^2 \end{bmatrix} \tag{7}$$

$${}^*Z = Z^T * (Z * Z^T)^{-1}$$

$$\begin{bmatrix} {\Omega_1}^2 \\ \vdots \\ {\Omega_8}^2 \end{bmatrix} = {}^*Z * \begin{bmatrix} F_t \\ M_r \\ M_p \\ M_y \end{bmatrix} \tag{8}$$

Here, ${}^*Z$ is the pseudo inverse of the Z matrix.

$$Z = \begin{bmatrix} k_f & k_f & k_f & k_f & k_f & k_f & k_f & k_f \\ \mathrm{A} * \mathrm{s}(\phi) & -\mathrm{A} * \mathrm{s}(\phi) & \mathrm{A} * \mathrm{c}(\phi) & \mathrm{A} * \mathrm{s}(\phi) & -\mathrm{A} * \mathrm{s}(\phi) & -\mathrm{A} * \mathrm{c}(\phi) & -\mathrm{A} * \mathrm{c}(\phi) & \mathrm{A} * \mathrm{c}(\phi) \\ \mathrm{A} * \mathrm{c}(\phi) & -\mathrm{A} * \mathrm{c}(\phi) & \mathrm{A} * \mathrm{s}(\phi) & -\mathrm{A} * \mathrm{c}(\phi) & \mathrm{A} * \mathrm{c}(\phi) & -\mathrm{A} * \mathrm{s}(\phi) & \mathrm{A} * \mathrm{s}(\phi) & -\mathrm{A} * \mathrm{s}(\phi) \\ k_m & k_m & -k_m & -k_m & -k_m & -k_m & k_m & k_m \end{bmatrix} \tag{9}$$

In this matrix, the angle ϕ is the angle between the axis of each arm to which the rotors are attached and the roll or pitch axes, which is 22.5 degrees for the eight-rotor UAV model. In order to write this matrix more simply, the abbreviation $A = k_f * l$ was made. Another moment is the gyroscopic moment, which is the moment caused by a change in the rotation axes of the rotors, depending on the mechanical properties of the propeller and rotors. Since the effect of gyroscopic moments in the z-axis is negligible, they are often ignored.

$$\mathrm{M}_x = -\sum_{i=1}^{\mathrm{n}} (-1)^i * (I_{zz} * \ p * \ \Omega_i) \tag{10}$$

$$\mathrm{M}_y = \sum_{i=1}^{\mathrm{n}} (-1)^i * (I_{zz} * \ q * \ \Omega_i) \tag{11}$$

In Equations 10 and 11, the effect of the gyroscopic effect on the x and y axes, that is, the roll and pitch moments are given. In these equations, I_{zz} is the inertia of the rotor in the axis of rotation, and p and q are the pitch and roll angular velocities, respectively, with respect to the body coordinate system.

The total moment (M_T) acting on the vehicle is obtained by summing the roll-pitch-yaw moments due to the lifting force produced by the propellers and the moments (M_{jr}) due to the gyroscopic effect, as given in Equation 12. M_r, M_p, and M_{yw} are the pitch, roll, and yaw moments, respectively.

$$\mathrm{M}_T = \begin{bmatrix} \mathrm{M}_r \\ \mathrm{M}_p \\ \mathrm{M}_{yw} \end{bmatrix} + \begin{bmatrix} \mathrm{M}_x \\ \mathrm{M}_y \\ 0 \end{bmatrix} \tag{12}$$

In summary, the simplified nonlinear model of the octorotor UAV is given below.

$$\begin{gathered} m\ddot{x} = -(F_t + w_x)sin\theta \\ m\ddot{y} = (F_t + w_y)cos\theta sin\varphi \\ m\ddot{z} = (F_t + w_z)cos\theta cos\varphi - mg \\ I_x\ddot{\theta} = \mathrm{M}_r + w_\theta \\ I_y\ddot{\varphi} = \mathrm{M}_p + w_\varphi \\ I_z\ddot{\psi} = \mathrm{M}_{yw} + w_\psi \end{gathered} \tag{13}$$

where x, y, and z denote the position of the vehicle, φ, θ, and ψ are the roll, pitch and yaw angles, respectively, I_j represents the inertia matrix in the j-axis, and g is the gravitational acceleration. Correspondingly, w_i, where *i* takes values x, y, z, ψ, θ or ϕ, denotes the unknown disturbances.

2.2. Adaptive Landing Gear System

The landing gear system consists of four arms. Each arms have two limbs and thus has two degrees of freedom and has a simple mechanical structure. In Fig. 2, it is aimed to define the kinematic structure with an arm of the landing gear.

The kinematic equations of the robot arm are obtained as follows, considering the structure of the commonly known two-joint planar manipulator. Equation 14 can find the position of the edge point $P\ (x, y)$ of the arm by considering the limb lengths and joint angles. Which are referred to as forward kinematic equations. If it is necessary to find joint angles corresponding to the desired position of this endpoint, then inverse kinematics operation is required. This is obtained as in Equation 15.

$$\begin{gathered} P_x = l_1\, cos(\theta_1) + l_2\, cos(\theta_1 + \theta_2) \\ P_y = l_1\, sin(\theta_1) + l_2\, sin(\theta_1 + \theta_2) \end{gathered} \tag{14}$$

$$\begin{gathered} \theta_2 = cos^{-1}((P_x{}^2 + P_y{}^2 - l_1{}^2 - l_2{}^2)/2l_1l_2) \\ \theta_1 = atan2\big(P_y, P_x\big) - atan2(l_2\, sin(\theta_2)\,, (l_1 + l_2\, cos(\theta_2))) \end{gathered} \tag{15}$$

It has been emphasized before that the safe landing of the UAV is a very important issue. For this

reason, the adaptive landing gear must act sensitively with respect to the ground when the drone will land on different textured ground.

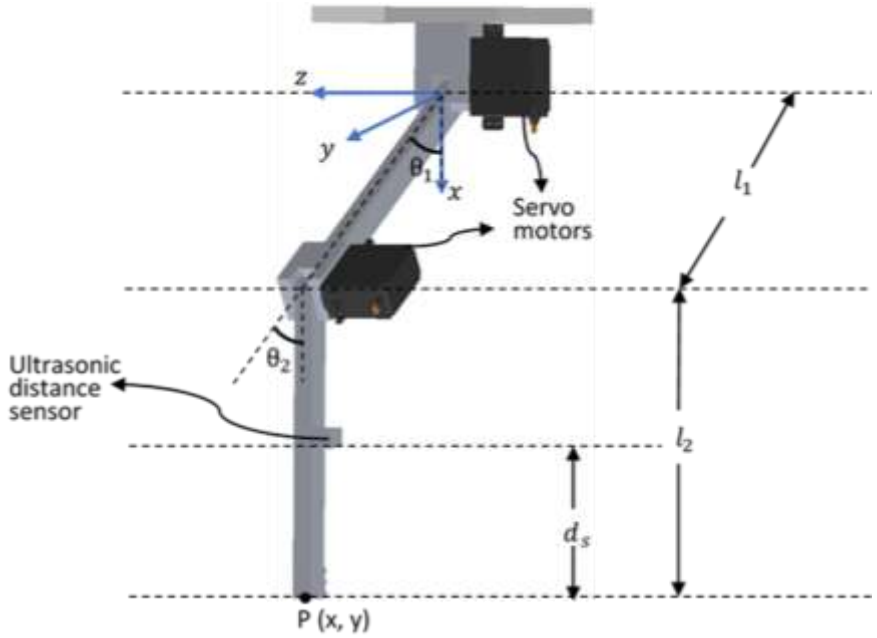

Figure 2. One robot arm structure for adaptive landing gear.

The UAV can either land on a flat ground or land on a sloping ground by keeping its body straight, or it can land on a sloping ground with a certain angle of inclination of its body. The visuals that exemplify these situations are given in Figure 3. The kinematic equations of the adaptive landing gear were obtained by considering an image showing the UAV landing on a sloping ground.

In Figure 4, the case of the UAV landing on a ground with β inclination angle with γ hull inclination angle is illustrated. For a safer landing, the part of the arm that contacts the ground, the second limb, is assumed to always have an orientation perpendicular to the ground. Thus, the kinematic equations of the landing gear are obtained by considering only the first joint angle. In the figure and equations, r_1 and r_2 are the perpendicular distances between the axis of gravity (CoG) where the center of mass of the vehicle is located and the contact points of the opposite arms with the ground. In the same order, h_1 and h_2 are the perpendicular distances between the ground contact point of the opposite arms and the vehicle's center of mass (CoM).

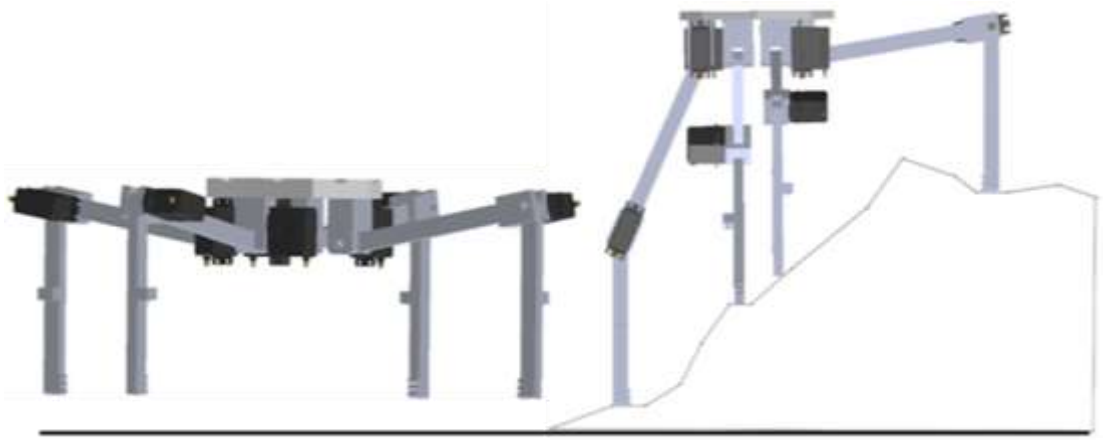

(a) (b)

Figure 3. Position of the landing gear on level ground (a) and on sloping ground (b).

These values are used to calculate the slope angle of the sloping ground as seen in Equation 16. The angle that the vehicle body makes with the horizontal axis, γ, is measured in the inertial measurement unit (IMU). The maximum angle (ϕ) of inclination of the inclined surface on which the vehicle can land is given in Equation 16.

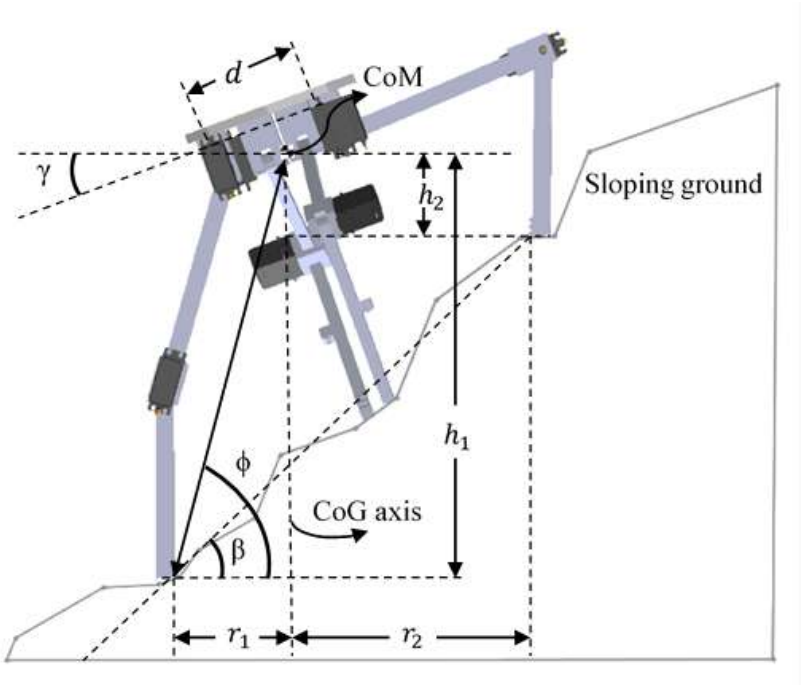

Figure 4. Schematic view of the landing gear for kinematic analysis.

$$\phi = \beta + \gamma \tag{16}$$

By keeping the vehicle body flat, in which case the γ angle value is zero, the position limits that the landing gear can take for the vehicle to land on a ground can be determined by considering the image as seen in Figure 5.

Here, α is the angle made by the first member of one arm of the landing gear in the opposite

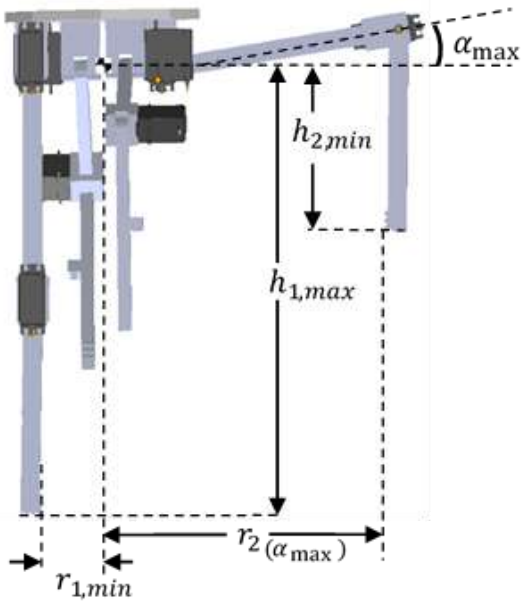

Figure 5. Display of position limits on the landing gear.

direction to the horizontal axis. The limit of this angle is determined in such a way that the first limb does not touch the arms to which the propellers of the vehicle are attached.

$$\begin{aligned} r_1 &= \left(\frac{d}{2}\right)\cos\gamma + l_1\sin(\theta_1 - \gamma) \\ r_2 &= \left(\frac{d}{2}\right)\cos\gamma + l_1\sin(\theta_1 + \gamma) \\ h_{1,max} &= \left(\tfrac{d}{2}\right)\sin\gamma + l_1\cos(\theta_1 - \gamma) + l_2 \\ h_1 &= \left(\frac{d}{2}\right)\sin\gamma + l_1\cos(\theta_1 - \gamma) + l_2 \\ h_2 &= \left(\frac{d}{2}\right)\sin\gamma + l_1\cos(\theta_1 + \gamma) + l_2 \end{aligned} \tag{17}$$

$$\begin{aligned} R &= r_1 + r_2 \\ \Delta h &= h_1 - h_2 \\ \tan\beta &= \Delta h/R \\ \beta &= \mathrm{Atan2}(\Delta h, R) \end{aligned} \tag{18}$$

$$h_{2,min} = \left(\frac{d}{2}\right)\sin\gamma + l_1\cos(\theta_1 - \gamma) + l_2 - l_1\sin\alpha$$

$$\begin{aligned} r_{1,min} &= \left(\tfrac{d}{2}\right)\cos\gamma + l_1\sin(\theta_1 - \gamma) \\ r_{2,min} &= \left(\frac{d}{2}\right)\cos\gamma + l_1\sin(\theta_1 - \gamma) - (l_1 - l_1\cos\alpha) \end{aligned} \tag{19}$$

In addition, in relation to the physical characteristics of the landing gear, the boundaries of the vertical distances between the ground contact points of the second limbs of the opposing arms and the vehicle's center of gravity are determined. In this context, the values $h_{1,max}$ and $h_{2,min}$ are calculated.

$$\begin{aligned} \Delta h_{max} &= h_{1,max} - h_{2,min} \\ R_{min} &= r_{1,min} + r_{2,min} \end{aligned} \tag{20}$$

Limit values can be found by considering the values in Table 1 where the physical characteristics of the vehicle are given.

Table 1. Physical dimensions of the landing gear.

Parameters	Descriptions	Unit	Value
l_1	First limb length	[mm]	200
l_2	Second limb length	[mm]	200
d	Perpendicular distance between the axis of rotation of the first joints	[mm]	100
d_s	The distance of the sensor to the end point of the second limb	[mm]	100
α_{max}	Maximum angle value of the first joint in the opposite direction	[°]	10

Using the difference between these values, Δh_{max}, and similarly, R_{min}, which is the vertical distance value between the contact points of the second limbs of the opposite arms with the ground, the maximum value of the inclination angle of the ground on which the vehicle can land is calculated using Equations 19 and 20. This angle is calculated assuming the vehicle body is parallel to the horizontal. Which requires that the angle γ in Figure 4 be zero. In this case, if the vehicle body leans by an angle of γ, the tilt angle ϕ, at which the vehicle can stop without tipping over, must be less than 90 degrees. When Figure 5 is examined, it can be seen that $\phi = atan2\,(r_{1,min}\,, h_{1,max})$.

According to the values given in the table, the angle of inclination of the sloping ground on which the UAV can land can be calculated as follows.

For α=α_{max} and γ=0; $h_{1,max}$= 400 mm, $h_{2,min}$=131.6 mm, $r_{1,min}$= 50 mm, $r_{2,min}$=223.2 mm

Thus, Δh_{max}= 268.4 mm and R_{min}=273.2 mm. By using these limit values, β=44.5°, which is the maximum slope angle of the ground; Which is the limit value when the UAV body is desired to be parallel to the horizontal axis (γ=0). According to these physical values of the adaptive landing gear, it shows that the UAV can safely land on uneven ground with a sloping angle of 44.5°.

3. Control Principle and Simulation of the Adaptive Landing Gear System

The control of the proposed adaptive landing gear is based on four ultrasonic distance sensors on the robot arms. The distance information received from the sensors is converted into real distance data according to the location of the sensor, which is given as d_s. Since the robot arm with the least of these real distances will be the closest to the ground, this arm will be the reference for the other arms.
Δd_i (for i:1 to 4), which is the difference between this reference value and the actual distance values measured from other sensors, will be the basic data for the control of the servo motors in the arms. According to this data, the robot arm joint angles are changed so that the end point of all four limbs of the landing gear is the same distance from the ground. This process continues until the actual distance data calculated by measuring from four different sensors becomes zero. When the zero value is reached, the landing is completed.

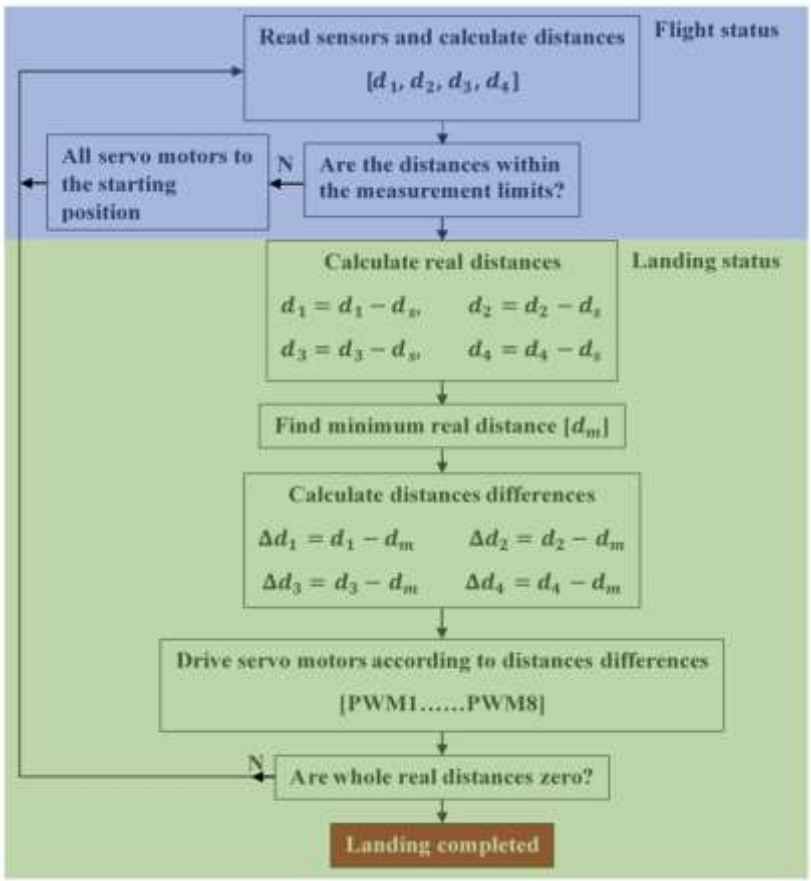

Figure 6. Flow chart of the adaptive landing gear controller.

If the distance data measured from the sensors is outside the determined distance limit, it will mean that the UAV is not yet in the landing process, so the servo motors on the landing gear will remain in the starting position. The flow chart describing this process is given in Figure 6.

The block diagram of the simulation study of the proposed system is given in Figure 7. In case of experimental work, it will be sufficient to transfer this control system to the hardware. As can be seen from the block diagram, the distance data received from four ultrasonic sensors are processed to produce Pulse Width Modulated (PWM) signals for servo motors.

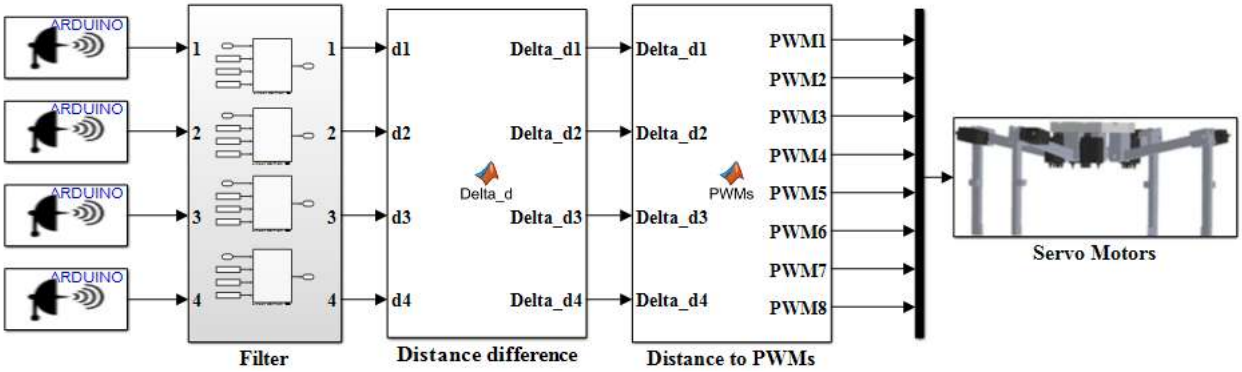

Figure 7. Matlab Simulink diagram of adaptive landing gear system control.

In a sample simulation study, the variation of the joint angles with respect to time and the positions of the robot arm endpoints according to these angles are obtained and are given in Figure 8.

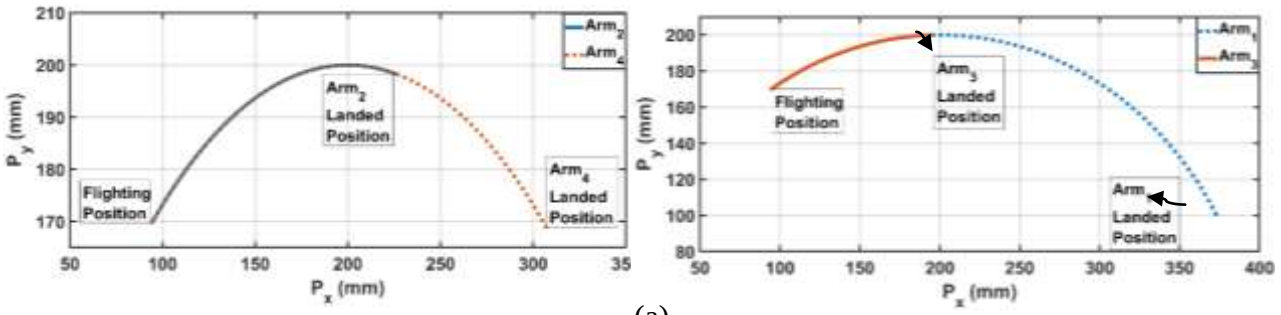

(a)

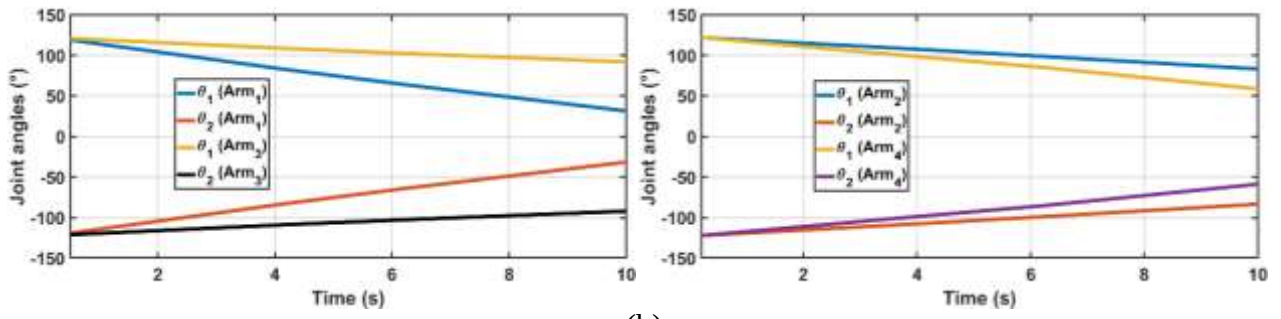

(b)

Figure 8. Changes in the positions of the endpoints of the four arms (a) and their corresponding joint angle changes (b).

In the same simulation study, the motion trajectories of the robot arm endpoints were obtained in three dimensions as seen in Figure 9. Representationally, after landing, the inclination angles of the UAV are shown by geometrically correlating the arm endpoints.

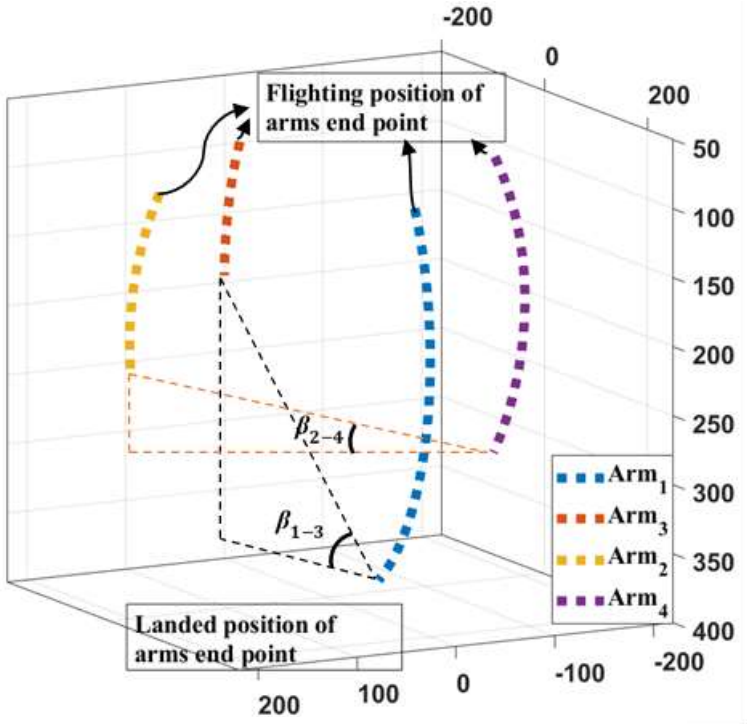

Figure 9. Trajectory of motion of the endpoints of the four arms and their inclination in both directions.

4. Conclusions

An adaptive landing gear design and kinematic analysis were performed for an Octorotor UAV. Ultrasonic distance sensors were used to position the designed landing gear according to the uneven ground. Thus, provided that the physical dimensions of the landing gear are limited, the instantaneous surface slope of the UAV at the time of landing is calculated according to the slope of the inclined surface. A flowchart has been created for the control of adaptive landing gear. For this landing gear, which can be designed for UAVs with different physical structures, the maximum angle of inclination of the ground on which the vehicle can land safely was calculated as 44.5 degrees. This value is directly related to the length of the limbs of the arms (l_1 and l_2) and the distance between the junctions of these arms (d). In the landing gear designed within the scope of this study, these values were determined as l_1=200mm, l_2=200 mm and d=100 mm.

In addition to the conclusion that this proposed landing gear is applicable by simulation and calculations, it can be said that more realistic results can be obtained with experimental studies.

Authors' Contributions

NC carried out the analysis and studies in the article and wrote the article. He read and approved the final version of the article.

Competing Interests

The authors declare that they have no competing interests.

References

[1] Ahirwar, S., Swarnkar, R., Bhukya, S., Namwade, G., Application of Drone in Agriculture,

Int. J. Curr. Microbiol. Appl. Sci., 2019, 8 (1) 2500–2505.
[2] Wu, K., Rodriguez, G.A., Zajc, M., Jacquemin, E., Clément, M., De Coster, A., Lambot, S., A New Drone-Borne GPR for Soil Moisture Mapping, Remote Sens. Environ., 2019, 235, 111456.
[3] Liu, Y., Noguchi, N., Okamoto, H., Ishii, K., Development of A Small-Sized and Low-Cost Attitude Measurement Unit for Agricultural Robot Application, Tarim Bilim. Derg., 2018, 24 (1), 33–41.
[4] Liu, S., Dong, W., Ma, Z., Sheng, X., Adaptive Aerial Grasping and Perching with Dual Elasticity Combined Suction Cup, IEEE Robot. Autom. Lett., 2020, 5 (3), 4766–4773.
[5] Villa, D.K.D., Brandão, A.S., Sarcinelli-Filho, M., A Survey on Load Transportation Using Multirotor UAVs, J. Intell. Robot. Syst. Theory Appl., 2020, 98, 267–296.
[6] Bonyan Khamseh, H., Janabi-Sharifi, F., Abdessameud, A., Aerial manipulation—A literature Survey, Rob. Auton. Syst., 2018, 107, 221–235.
[7] Ribeiro, M., Ferreira, A.S., Goncalves, P., Galante, J., de Sousa, J.B., Quadcopter Platforms for Water Sampling and Sensor Deployment, in: Ocean., 2016 MTS/IEEE Monterey, IEEE, 2016, 1–5.
[8] Şen, M.A., Bakırcıoğlu, V., Kalyoncu, M., Inverse Kinematic Analysis Of A Quadruped Robot, Int. J. Sci. Technol. Res., 2017, 6 (09) 285–289.
[9] Yıldırım, Ş., Arslan, E., A Comparison of Six Legged ODE (Open Dynamics Engine) Based Gait control Algorithm and Standard Walking Gaits, Avrupa Bilim ve Teknoloji Dergisi , Özel Sayı, 2019, 242-255.
[10] Ersin, Ç., Yaz, M., Gökçe, H., Upper Limb Robot Arm System Design and Kinematic Analysis, El-Cezeri J. Sci. Eng., 2020, 7 (3) 1320–1331.
[11] DARPA, Robotic Landing Gear Could Enable Future Helicopters to Take Off and Land Almost Anywhere, 2015. [https://www.darpa.mil/news-events/2015-09-10 (accessed June 7, 2021)].
[12] Sarkisov, Y.S., Yashin, G.A., Tsykunov, E. V., Tsetserukou, D., DroneGear: A Novel Robotic Landing Gear with Embedded Optical Torque Sensors for Safe Multicopter Landing on an Uneven Surface, IEEE Robot. Autom. Lett., 2018, 3 (3) 1912–1917.
[13] Luo, C., Zhao, W., Du, Z., Yu, L., A Neural Network Based Landing Method for an Unmanned Aerial Vehicle with Soft Landing Gears, Appl. Sci., 2019, 9 (15), 2976.
[14] Çabuk, N., Bakırcıoğlu, V., Artificial Neural Networks Based Inverse Kinematics Solution and Simulation of a Six Degree of Freedom Lighting Manipulator, Gazi Univ. J. Sci. Part C Des. Technol., 2018, 6 (1) 117–125.
[15] Yildirim, Ş., Design of a Proposed Neural Network Control System for Trajectory Controlling of Walking Robots, Simul. Model. Pract. Theory., 2008, 16 (3) 368–378.
[16] Nadan, P.M., Anthony, T.M., Michael, D.M., Pflueger, J.B., Sethi, M.S., Shimazu, K.N., Tieu, M., Lee, C.L., A Bird-Inspired Perching Landing Gear System, J. Mech. Robot., 2019, 11 (6), 061002.
[17] Tang, H., Zhang, D., Gan, Z., Control System for Vertical Take-Off and Landing Vehicle's Adaptive Landing Based on Multi-Sensor Data Fusion, Sensors (Switzerland)., 2020, 20 (16) 1–21.